

*J. L. Goldberg 622*

SIXTH QUARTERLY REPORT  
FOR  
A DAY-NIGHT HIGH RESOLUTION INFRARED  
RADIOMETER EMPLOYING TWO-STAGE RADIANT COOLING

(1 July 1967 - 1 October 1967)

Contract No. NAS 5-10113

FACILITY FORM 602	<b>N68-17435</b>	
	(ACCESSION NUMBER)	(THRU)
	<i>45</i>	<i>1</i>
	(PAGES)	(CODE)
	<i>OK-93291</i>	<i>14</i>
	(NASA CR OR TMX OR AD NUMBER)	(CATEGORY)

Prepared by

ITT Industrial Laboratories  
Fort Wayne, Indiana 46803

For

National Aeronautics and Space Administration  
Goddard Space Flight Center  
Greenbelt, Maryland 20771

GPO PRICE	\$	
CFSTI PRICE(S)	\$	
Hard copy (HC)		<i>3.00</i>
Microfiche (MF)		<i>.65</i>

ff 653 July 65

ITTIL No. 67-1046

15 September 1967

SIXTH QUARTERLY REPORT  
FOR  
A DAY-NIGHT HIGH RESOLUTION INFRARED  
RADIOMETER EMPLOYING TWO-STAGE RADIANT COOLING

(1 July 1967 - 1 October 1967)

Contract No. NAS 5-10113

Prepared by

ITT Industrial Laboratories  
Fort Wayne, Indiana 46803


For

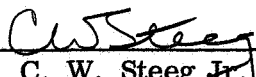
National Aeronautics and Space Administration  
Goddard Space Flight Center  
Greenbelt, Maryland 20771

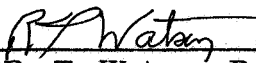
Contributors

R. V. Annable and J. F. Lodder

Approved by

  
K. L. DeBrosse, Manager  
Space and Applied Science Dept.

  
Dr. C. W. Steeg Jr., Director  
Product Development

  
Dr. R. T. Watson, President  
ITT Industrial Laboratories

## ABSTRACT

This report describes the completion of tests on the two-stage radiant cooler to be used in a 10.5 to 12.5 micron Day-Night High Resolution Infrared Radiometer and the initiation of construction on a breadboard radiometer. Thermal tests were made on single- and two-stage radiant coolers with aluminized mylar cone walls. Construction of the scan head and optics for the breadboard radiometer was begun and assembly of the necessary thermal and electronic test equipment continued.

The feasibility of the two-stage radiant cooler was demonstrated under realistic thermal and mechanical conditions. The second-stage patch attained a temperature near 77 degrees K when corrected for a minimum cold space reference reflectivity of 2 percent. The accuracy of temperature measurements is presently limited by the reflection of radiation from the first-stage cone to the patches by way of the flat space reference. It is recommended that the reflectivity be reduced by providing cavities in the surface of the space reference.

## TABLE OF CONTENTS

	Page
1.0 INTRODUCTION -----	1
2.0 THERMAL TESTS -----	2
2.1 Single-Stage Radiant Cooler -----	2
2.2 Two-Stage Radiant Cooler -----	6
2.3 Radiative Transfer Parameters -----	12
2.3.1 First Stage -----	13
2.3.2 Second Stage -----	14
2.4 Temperature Corrections for Imperfect Space Reference	16
2.4.1 Space Reference Temperature -----	16
2.4.2 Space Reference Reflectivity -----	17
2.4.3 Reduction of Temperature Corrections -----	25
3.0 BREADBOARD RADIOMETER -----	27
3.1 Scan Head -----	27
3.2 Relay Optics -----	29
3.3 Electronics -----	31
3.4 Test Equipment -----	33
4.0 NEW TECHNOLOGY -----	37
5.0 PROGRAM FOR NEXT QUARTER -----	38
6.0 CONCLUSIONS AND RECOMMENDATIONS -----	39



# LIST OF ILLUSTRATIONS

		Page
Figure 1	Radiant Cooler Test No. 6 -----	4
Figure 2	Photograph of First-Stage Cone -----	7
Figure 3	Photograph of First-Stage Patch and Second-Stage Cone -	8
Figure 4	Photograph of First- and Second-Stage Patches -----	9
Figure 5	Radiant Cooler Test No. 7 -----	11
Figure 6	Photograph of Radiometer Scan Head -----	28
Figure 7	Relay Optics Assembly -----	30
Figure 8	Preamplifier Broadband Noise Performance -----	32
Figure 9	Test Equipment Block Diagram -----	34
Figure 10	Photograph of Electronic Test Equipment -----	35
Figure 11	Photograph of Space Scan and Calibration Targets in Space Chamber -----	36

# LIST OF TABLES

		Page
Table 1	Single-Stage Measurements Corrected for Reference Reflectivity -----	5
Table 2	Emissivities Corrected for Reference Reflectivity -----	5
Table 3	Two-Stage Corrections for Reference Reflectivity -----	10
Table 4	Two-Stage Measurements Corrected for Reference Reflectivity -----	12
Table 5	Parameters Used to Predict $T_{p1}$ -----	13
Table 6	First-Stage Patch Temperatures -----	14
Table 7	Calculation of $\epsilon_{pc}^{(2)}$ -----	15
Table 8	Estimate of Cone Surface Emissivity in Second Stage -----	15
Table 9	View Factor to First n-1 Reflections of Second-Stage Patch -	19
Table 10	Calculation of $g_{oc}$ for $\rho_g = 0.93$ -----	20
Table 11	Results of Thermal Test 7 -----	20
Table 12	Radiant Power Reflected from Space Reference -----	21
Table 13	Conductive Members Between Stages in Test 7 -----	22
Table 14	Thermal Load on Second-Stage Patch for Reference Reflections to First Stage Only -----	23
Table 15	Temperature of Second-Stage Patch for Reference Reflections to First-Stage Only -----	23
Table 16	Thermal Load on First-Stage Patch Reflected from Space Reference -----	24
Table 17	Outer Space Temperature of First-Stage Patch -----	24
Table 18	Outer Space Temperature of Second-Stage Patch -----	25
Table 19	Properties of a $30^\circ$ V-Groove Cavity -----	26
Table 20	Required Radiometer Characteristics -----	27
Table 21	Relay Optics Design -----	29
Table 22	Preamplifier Specifications -----	31
Table 23	Electronic Test Equipment -----	33

## 1.0 INTRODUCTION

This report covers the technical aspects of the work performed in the development of a two-stage radiant cooler and associated 10.5 to 12.5 micron day-night radiometer during the quarterly period from 1 July 1967 to 1 October 1967. During the reporting period, thermal testing of the two-stage radiant cooler was completed, and construction of the breadboard radiometer was started. The thermal tests demonstrated the feasibility of the two-stage radiant cooler under realistic thermal and mechanical conditions. A second-stage temperature near 77 degrees K was obtained when readings were corrected for the minimum cold space reference reflectivity of 0.02. Analysis of the temperature measurements showed that the cone walls have an emissivity of  $0.070 \pm 0.007$  over the possible range of space reference reflectivity. Temperature corrections are necessary because of the imperfect space reference, largely as a result of non-zero reflectivity. The corrections can be reduced by providing cavities in the reference surface.

The second phase of the program, construction and testing of a vibrationally sound two-stage cooler, was approved by the Technical Officer on 11 September 1967. The third phase of the program, integration of the radiant cooler with a working breadboard radiometer of specific characteristics, was begun on the same date. Construction of the scan head and optics was started and assembly of the test equipment continued.

A 10.5 to 12.5 micron instrument permits radiometric mapping of the earth and its cloud cover both day and night. It is an extension of the 3.4 to 4.2 micron nighttime High Resolution Infrared Radiometer flown on Nimbus I and II. The two-stage radiant cooler is an extension of the single-stage cooler employed on the Nimbus radiometer.

## 2.0 THERMAL TESTS

The feasibility of the two-stage radiant cooler was demonstrated during thermal test 7 conducted on August 28 and 29. The results of this test are covered in Sections 2.2 and 2.3. When corrected for the minimum cold reference reflectivity of 2 percent, the second-stage patch attained a temperature near 77 degrees K. The heat load conditions were made realistic by operating the first-stage cone near its expected in-orbit temperature. The orbital cone temperature had been estimated for a Nimbus-type orbit at an altitude of 600 nautical miles and an orbit normal to sun angle of 79 degrees (See Fifth Quarterly Report, Section 4.3). Realistic mechanical conditions in critical cooler parts were insured by the successful vibration tests conducted last May (Fifth Quarterly Report, Section 2.0).

The accuracy of simulation of orbital operation is presently limited by the reflection of radiation from the first-stage cone to the first- and second-stage patches by way of the flat cold space reference (Section 2.4). For a nominal reference reflectivity of 5 percent, the total increase in the temperature of the second-stage patch is about 8 degrees K. The error produced by a reference temperature of 30 degrees K, which is above that of outer space (4 degrees K), is negligible by comparison. The reflectivity of the space reference can be reduced (absorptivity increased) by the use of the cavity effect, e. g., by covering the surface with triangular grooves.

Analysis of thermal test 6 on a single-stage radiant cooler (Sections 2.1 and 2.3.1) shows that the emissivity of the cone surface (aluminized mylar) is  $0.070 \pm 0.007$  when corrected for a space reference reflectivity of  $0.05 \pm 0.03$ . Analysis of thermal test 7 on a two-stage cooler (Sections 2.2 and 2.3.1) shows that the performance of the first-stage patch in a two-stage cooler can be accurately predicted from data on a single-stage cooler.

Estimates of radiative transfer parameters are less accurate in the second-stage (Section 2.3.2). The error introduced by the imperfect cold space reference is larger, and the geometry of the patch-cone structure is more complex. For the nominal reference reflectivity of 0.05, the estimated cone surface (aluminized mylar) emissivity in the second stage is 0.067, which is close to the first-stage value.

### 2.1 Single-Stage Radiant Cooler

Following thermal test 4 on a two-stage cooler (Section 2.2), the ambient sensor in the test rack was attached to the same board as the reference thermocouple junctions (on the multi-channel recorder). The sensor had previously been located on the cabinet about a foot below the reference junctions. A second test of a two-stage cooler model (thermal test 5) was then begun. The only change from test 4 was supposed to be that the inside surface of the second-stage cone had been lined with aluminized mylar. When it became apparent that the first-stage (which was unchanged) was not cooling as well as previously, the test was terminated.

Examination of the cooler showed that it had not been properly assembled, i. e., changes had been made in addition to the attachment of the aluminized mylar in the second-stage cone. In addition, the 3M Black Velvet coating on the copper space reference had been damaged. The bolt heads protruding from the copper had been scraped; other areas of the black coating had been scratched and wiped.

Finally, relocation of the ambient sensor showed that a significant temperature difference could exist between the thermocouple reference junctions and the original position of the ambient sensor. This made the results of all previous thermal tests questionable. We therefore repeated the thermal test of the single-stage cooler with aluminized mylar attached to the cone walls (test 3). This time the ambient sensor was attached to the input board for the thermocouple wires. In addition, a blower was installed above the recorder to reduce temperature gradients in the test rack and to prevent high reference junction temperatures (and therefore large corrections when calculating thermocouple outputs referenced to 0 degrees C). Finally, the copper reference was repainted and the bolts replaced with countersunk flat head screws.

Test 6 on a single-stage radiant cooler with aluminized mylar cone walls (repeat of test 3) was conducted on August 21 and 22. The temperature measurements are shown in Figure 1. The cooler attained the following equilibrium temperatures (averages of 8 readings over a 5 hour period).

Outer box	288 degrees K
Cone	204.4 degrees K
Patch	105.1 degrees K

The Alzak surface on the inside wall of the box was covered with aluminized mylar to attain better simulation of in-orbit thermal conditions. The other three box surfaces facing the cone (all mill-finished aluminum) were not covered. The result was a cone temperature within the expected orbital range (203 degrees K to 206 degrees K, Fifth Quarterly Report, Section 4.3).

The equilibrium patch temperature was corrected for the affect of a non-black space reference (Fifth Quarterly Report, Section 4.5). The results are shown in Table 1 for space reference reflectivities of 8, 5, and 2 percent. The 3M Black Velvet coating probably has a reflectivity of about 5 percent for greybody radiation at the cone temperature,  $T_c$ .

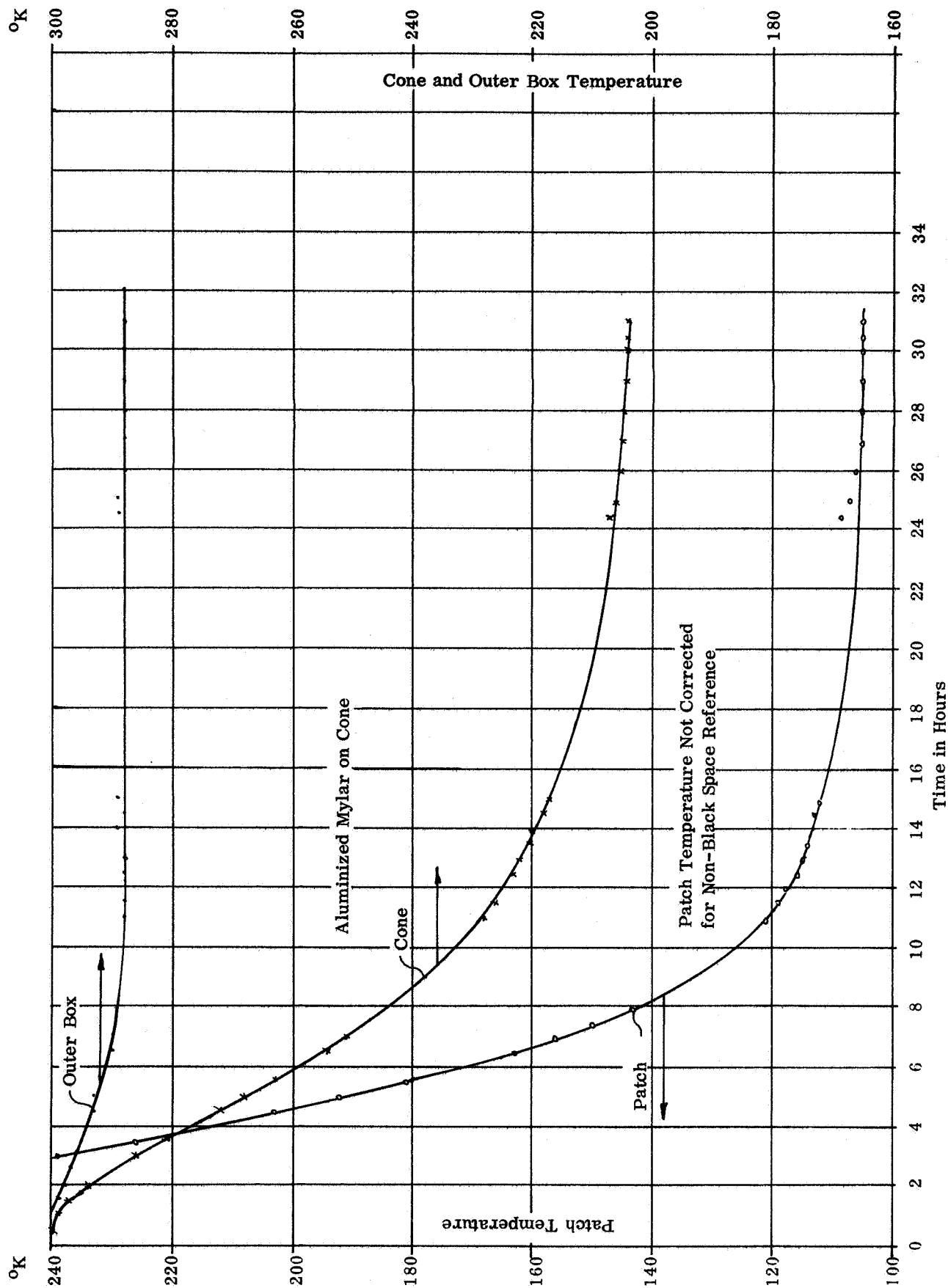


Figure 1 Radiant Cooler Test No. 6 (Aug. 21 & 22, 1967)

Table 1

## Single-Stage Measurements Corrected for Reference Reflectivity

Space Reference Reflectivity	Correction to Patch Temperature		Corrected Patch Temperature ( $T_p$ )	$T_p/T_c$
	%	$\Delta T_p$		
0.08	6.6	-6.9°K	98.2°K	0.4804
0.05	4.2	-4.4°K	100.7°K	0.4926
0.02	1.7	-1.8°K	103.3°K	0.5053

The value of  $T_p/T_c$  for test 3 was 0.481 (Fifth Quarterly Report, Table 1).  
Test 6 yielded a value of 2.4 percent higher for a reference reflectivity of 5 percent.

The effective patch-to-cone emissivity,  $\epsilon_{pc}$ , and the average emissivity of the cone surface,  $\epsilon_g$ , can be calculated from the  $T_p/T_c$  ratio (Fifth Quarterly Report, Section 4.2). The results are shown in Table 2 for the above three values of reference reflectivity, together with the results from Test 3. The cone surface emissivity for Test 6 is  $0.070 \pm 0.007$ .

Table 2

## Emissivities Corrected for Reference Reflectivity

Space Reference Reflectivity	$\epsilon_{pc}$	$\epsilon_g$
0.08	0.0533	0.0630
0.05	0.0589	0.0697
0.02	0.0652	0.0773
Test 3	0.0535	0.0632

The emissivities for a space reference reflectivity of 5 percent are 10 percent higher than those from test 3. Because of the fourth power dependence, errors and uncertainties in temperature are amplified when expressed in terms of emissivity.

During test 6, a thermocouple was used to monitor the temperature difference between the reference junctions and the original positions of the ambient sensor. The difference was relatively stable at about 1 degree C and never exceeded this value.

## 2.2 Two-Stage Radiant Cooler

Following the completion of thermal tests on single-stage models of the radiant cooler (reported in the Fifth Quarterly Report), a complete two-stage model was tested. Aluminized mylar was used to cover the inner surface of the first-stage cone and outer surface of the second-stage cone. The second-stage cone was molded of glass bead filled epoxy; its inner surface was covered directly with evaporated aluminum followed by evaporated gold.

The aluminized mylar was removed from the inner walls of the outer box to increase the thermal load on the first-stage cone and thereby more closely simulate in-orbit conditions (Fifth Quarterly Report, Section 4.3). However, this increased the cone temperature too much. Apparently the one Alzak surface on the inside of the box increased the radiative coupling more than expected.

The cooler temperatures at thermal equilibrium are listed below as measured and as corrected to an in-orbit cone temperature of 204 degrees K (see Fifth Quarterly Report, Section 4.3). These results should be considered approximate, however, because of the poor location of the ambient sensor during the test, as discussed below.

	As Measured	Corrected to Orbital Conditions
Outer Box	280°K	-
First-Stage Cone	211°K	204°K
First-Stage Patch	117°K	113°K
Second-Stage Patch	90°K	86°K

Following the test, the ambient sensor (platinum resistance thermometer) in the test rack was mounted on the input board of the multi-channel recorder (where the thermocouple wires are attached). The sensor had previously been located about a foot below the input board. We found a significant temperature difference between these locations when the equipment was operating. The average difference was about 4 degrees C, but varied as thermal conditions in the room changed. The above results for the fourth test were corrected for a nominal difference of 4 degrees K. However, the results are not entirely reliable, especially at low temperatures. For this reason, the test was repeated following a re-test of the single-stage cooler (test 6, Section 2.0).

The single-stage radiant cooler from thermal test 6 was changed to a two-stage model and tested on August 28 and 29. The outer and inner surfaces of the second-stage cone were covered with 0.5-mil aluminized mylar. Photographs of the two-stage radiant cooler are shown in Figures 2, 3, and 4. Figure 2 shows the first-stage cone. In Figure 3, half the first-stage cone has been removed to show the first-stage patch and second-stage cone. Figure 3 shows the first- and second-stage patches without the second-stage cone.



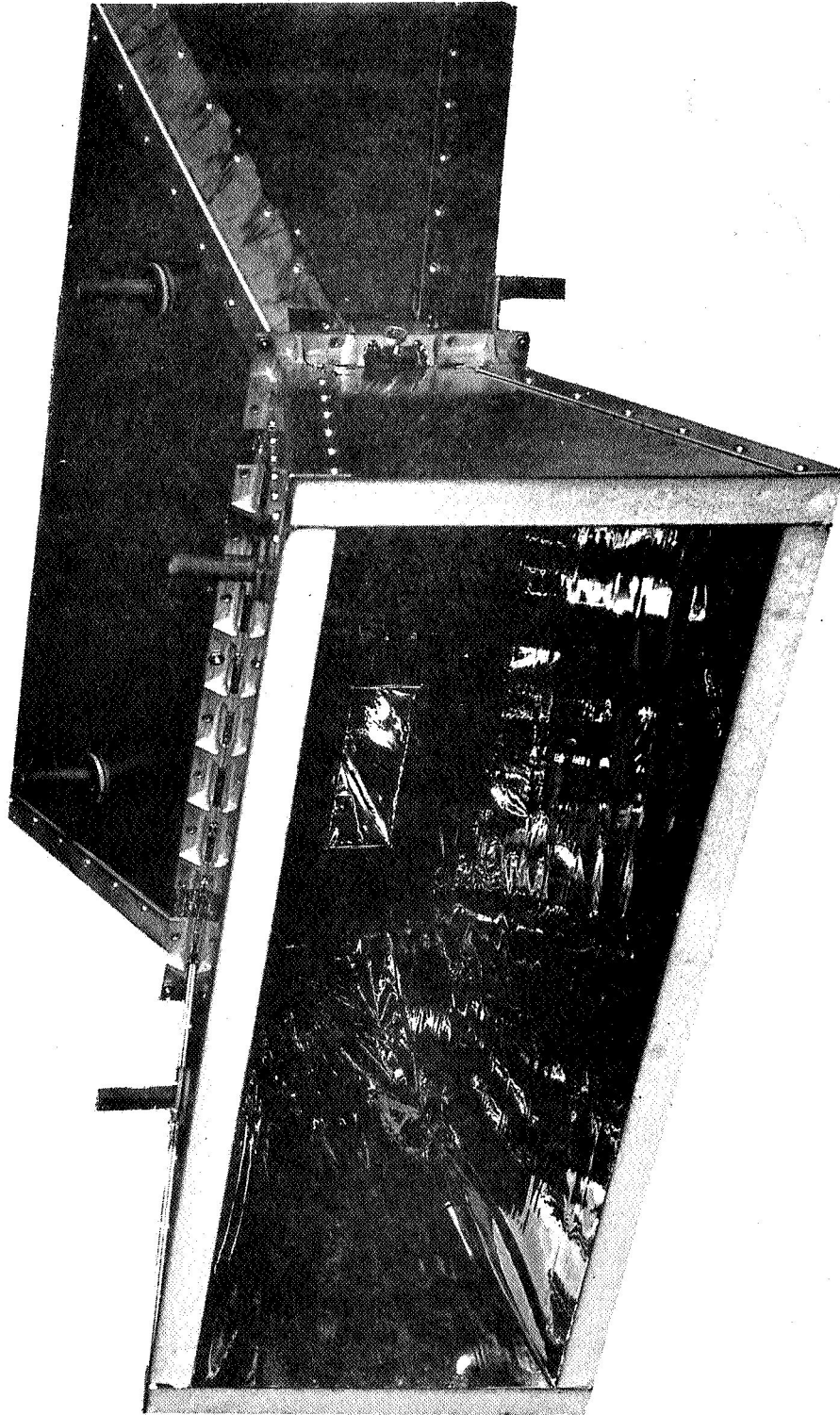


Figure 2 First-Stage Cone

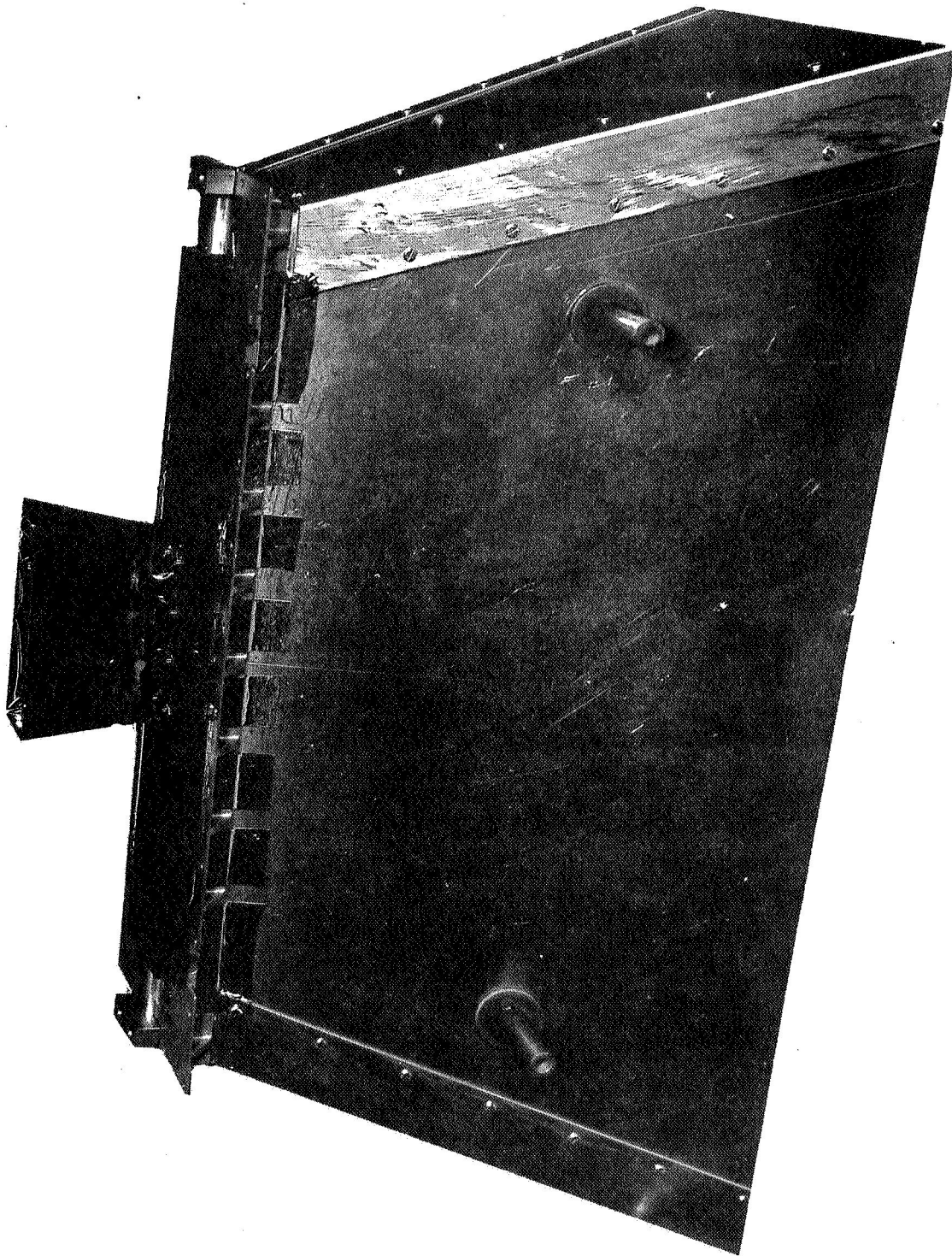


Figure 3 First-Stage Patch and Second-Stage Cone

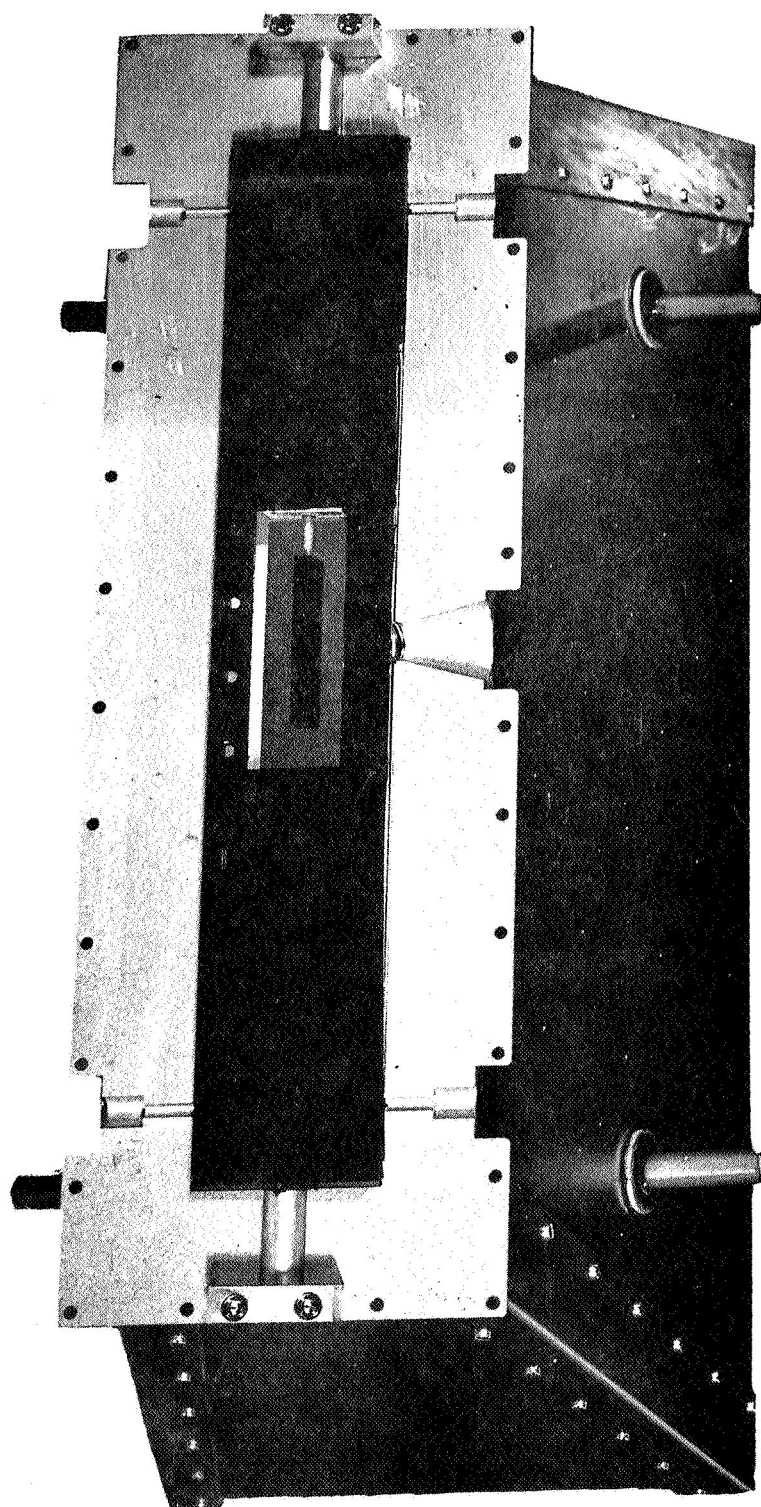


Figure 4 First- and Second-Stage Patches

As in test 6, the ambient sensor was attached to the same board as the reference thermocouple junctions. All thermocouples were calibrated by immersion in liquid nitrogen; chromel-alumel couples were used on the first-stage cone and patch and a chromel-constantan couple on the second-stage patch.

Temperature measurements during test 7 are shown in Figure 5. The two-stage radiant cooler attained the following equilibrium temperatures (average of 13 readings over a 5-1/2 hour period).

Outer box	289.5°K
First-stage cone	201.6°K
First-stage patch	108.3°K
Second-stage patch	80.2°K

The Alzak surface on the inside wall of the outer box was covered with aluminized mylar and the other inside surfaces were left uncovered. The result was, as in test 6, a cone temperature near the expected orbital range (Fifth Quarterly Report, Section 4.3).

The equilibrium patch temperatures were corrected for the effects of a non-black space reference. The temperature corrections are listed in Table 3 for reference (3M Black Velvet) reflectivities of 2, 5, and 8 percent. The detailed calculation of these corrections is given in Section 2.4.

Table 3

#### Two-Stage Corrections for Reference Reflectivity

Reference Reflectivity	Temperature Correction	
	First-Stage Patch	Second-Stage Patch
0.02	-1.1°K	-2.5°K
0.05	-2.9°K	-6.7°K
0.08	-4.8°K	-11.8°K

The temperature correction was first applied to the second-stage patch. The first-stage patch temperature was then corrected and the second-stage temperature ( $T_{p2}$ ) adjusted for the corrected first-stage temperature ( $T_{p1}$ ). Finally, the patch temperatures were determined for a first-stage cone temperature ( $T_c$ ) of 204 degrees K to permit better comparison with previous results (Fifth Quarterly Report, pp. 16 and 17; Section 2.4). The results are shown in Table 4.

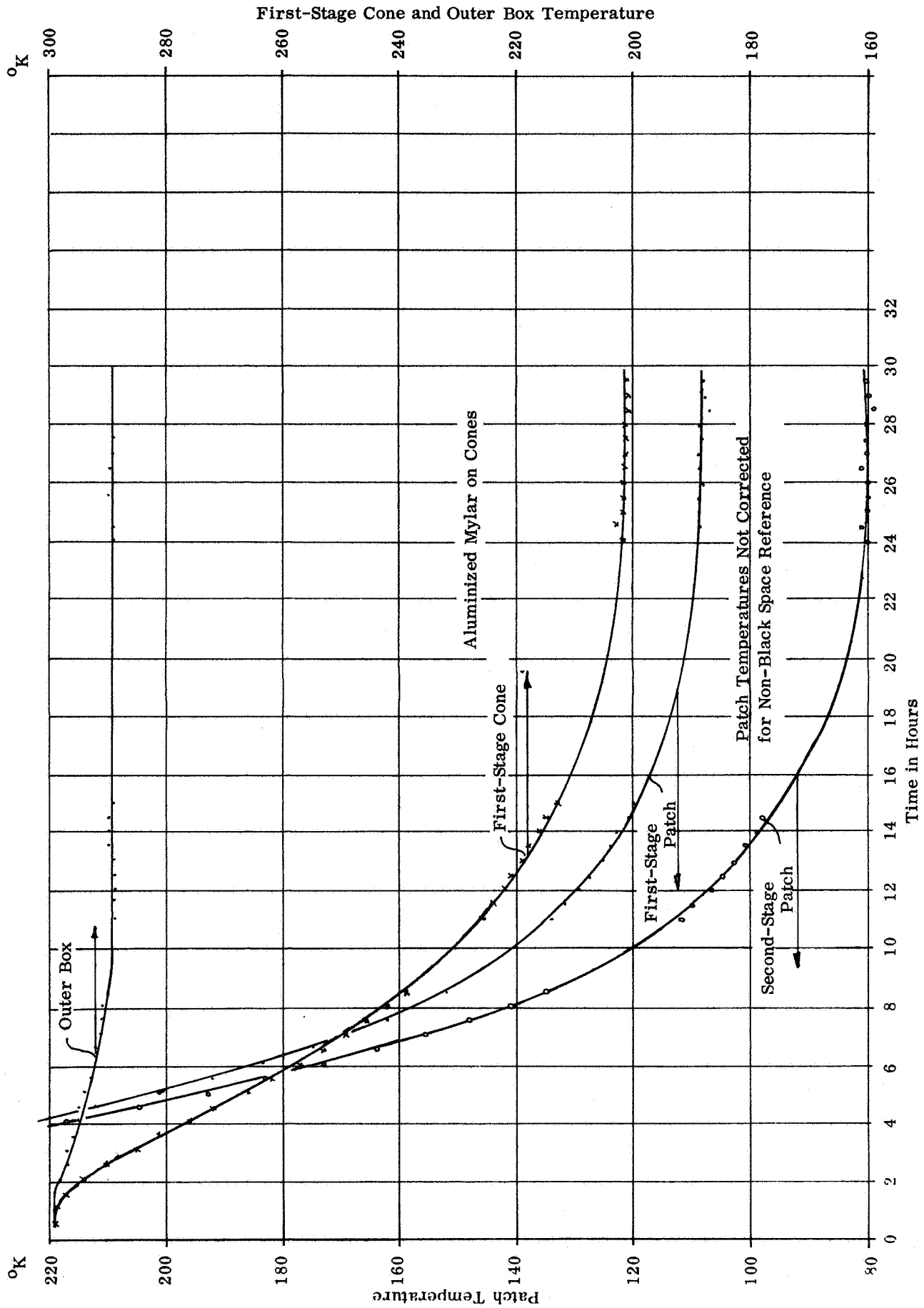


Figure 5 Radiant Cooler Test No. 7 (Aug. 28 & 29, 1967)

Table 4

## Two-Stage Measurements Corrected for Reference Reflectivity

Reference Reflectivity	Corrected Patch Temperatures			
	$T_c = 201.6^\circ\text{K}$		$T_c = 204^\circ\text{K}$	
	$T_{p1}$	$T_{p2}$	$T_{p1}$	$T_{p2}$
0.02	107.2 $^\circ\text{K}$	77.1 $^\circ\text{K}$	108.5 $^\circ\text{K}$	77.8 $^\circ\text{K}$
0.05	105.4 $^\circ\text{K}$	72.1 $^\circ\text{K}$	106.7 $^\circ\text{K}$	72.7 $^\circ\text{K}$
0.08	103.5 $^\circ\text{K}$	66.6 $^\circ\text{K}$	104.7 $^\circ\text{K}$	67.0 $^\circ\text{K}$

The first-stage patch temperature was calculated for the change in cone temperature using the direct proportionality between the temperatures of the first-stage patch and first-stage cone (First Quarterly Report, Eq. 79). The second-stage temperature was adjusted for changes in the first-stage temperature using the thermal balance equation for the second stage (First Quarterly Report, p. 54).

The non-black space reference introduces a total error in the second-stage temperature in the range 3.1 to 13.6 degrees K. The joule heating in the infrared detector produces a much smaller temperature increase. For example, the detector to be used in the breadboard radiometer has a resistance of 171 ohms and an optimum bias current (i. e., the current which gives the maximum detectivity) of 0.9 ma. The joule heating is then 0.1385 milliwatts. This additional power would increase the temperature of a second-stage patch from 72.1 degrees K to 72.8 degrees K. This is an increase of only 0.7 degrees K, which is much smaller than that produced by reflections off the space reference. Moreover, this result is for a 1/2 mm square detector. The use of smaller detectors in higher resolution instruments will further reduce the influence of joule heating. Since detector dissipation is proportional to its area, a 1/4 mm square detector, for example, would dissipate only about 0.04 milliwatts.

### 2.3 Radiative Transfer Parameters

The temperatures measured during thermal test 7 and corrected for space reference reflectivities of 2, 5, and 8 percent (Sections 2.2 and 2.4) were used to check the design equations of the first-stage patch and to estimate the radiative transfer parameters of the second stage. The radiative transfer parameters of the first stage determined from test 6 (Section 2.1) were used to predict the first-stage patch temperature in a two-stage cooler. The results were then compared with the measurements of test 7. This comparison was carried for space reference reflectivities of 2, 5 and 8 percent. The thermal balance equation for the second-stage patch was used to calculate the effective patch-to-cone emissivity and cone surface emissivity of the second stage.

The analyses of test results are useful for checking the design equations and for obtaining parameters to design other radiant coolers. However, it should be remembered that the prime objective was to attain the desired second-stage patch temperature under realistic thermal load conditions.

### 2.3.1 First Stage

The temperature of the first-stage patch in a two-stage radiant cooler is given by (First Quarterly Report, p. 48).

$$T_{p1} = (\epsilon'_{pc})^{1/4} T_c \quad (1)$$

where

$$\epsilon'_{pc} = \frac{\epsilon_{pc} (1 + \frac{1}{2} \frac{A_{c2}}{A_{p1}})}{1 + \frac{A_{c2}}{A_{p1}} [\epsilon_g + \epsilon_{pc} (1/2 - \epsilon_g)]} \quad (2)$$

$T_c$  = temperature of first-stage cone

$\epsilon_{pc}$  = effective patch-to-cone emissivity

$\frac{A_{c2}}{A_{p1}}$  = outside surface area of second-stage cone to surface area of first-stage patch

$\epsilon_g$  = emissivity of first-stage cone surface

The values of  $\epsilon_{pc}$  and  $\epsilon_g$  determined from thermal test 6 (single-stage cooler) are listed in Table 5 together with the calculated values of  $\epsilon'_{pc}$  for  $A_{c2}/A_{p1} = 0.810$ .

Table 5

Parameters Used to Predict  $T_{p1}$

Space Reference Reflectivity	$\epsilon_g$	$\epsilon_{pc}$	$\epsilon'_{pc}$
0.02	0.0773	0.0652	0.0844
0.05	0.0697	0.0589	0.0768
0.08	0.0630	0.0533	0.0700

The values of  $\epsilon'_{pc}$  were used to calculate the first-stage patch temperature from equation (1) for a first-stage cone temperature of 201.6 degrees K (attained in test 7). The results are given in Table 6 together with measured temperatures corrected to the same values of reference reflectivity (Table 4).

Table 6

## First-Stage Patch Temperatures

Space Reference Reflectivity	Predicted (°K)	Measured
0.02	108.7	107.2
0.05	106.1	105.4
0.08	103.7	103.5

On the average, the predictions are less than 1 percent from the corrected measurements.

2.3.2 Second Stage

Estimates of radiative transfer parameters are much less accurate in the second stage than in the first. The errors introduced by the imperfect cold space reference are larger in the second stage. In addition, an estimate of the cone surface emissivity requires the removal of the geometrical effects (multiple reflections). The original design equations were based on thin patches (i. e., they neglected the sides). This is a reasonable assumption for the first-stage patch but quite inaccurate for the second. Finally, the calculation of transfer parameters involves a temperature measurement raised to the fourth power. Errors in temperature measurements are therefore amplified when the results are expressed as transfer parameters.

Reasonably accurate estimates of the radiative transfer parameters from experimental temperature measurements are possible only in the first stage. A range of values can be calculated for the second stage, but the spread is somewhat larger. Such a range of values was determined by use of a weighting factor to account for the greater patch-to-cone interaction of the side areas of the second-stage patch.

The thermal balance equation for the second-stage patch (First Quarterly Report, p. 54) may be solved for the effective patch-to-cone emissivity of the second stage.

$$\epsilon_{pc}^{(2)} = \frac{\sigma A_{p2} T_{p2}^4 - K_c (T_{p1} - T_{p2})}{\sigma A_{p2} T_{p1}^4} \quad (3)$$

where  $A_{p2}$  = surface area of second-stage patch = 2.62 in<sup>2</sup>

$T_{p2}$  = temperature of second-stage patch

$K_c$  = conductive coupling coefficient between stages = 0.0356 mw/°K



The measured patch temperatures for thermal test 7 corrected to reference reflectivities of 2, 5, and 8 percent are listed in Table 7 together with the values of  $\epsilon_{pc}^{(2)}$  from equation (3).

Table 7

Calculation of  $\epsilon_{pc}^{(2)}$

Space Reference Reflectivity	$T_{p1}$ (°K)	$T_{p2}$	$\epsilon_{pc}^{(2)}$
0.02	107.2	77.1	0.1829
0.05	105.4	72.1	0.1187
0.08	103.5	66.6	0.0520

The calculation of  $\epsilon_{pc}^{(2)}$  from the surface emissivity of the cone,  $\epsilon_g^{(2)}$ , is covered in Appendix III to the First Quarterly Report. The calculation is for a thin patch. For values of  $\epsilon_g^{(2)}$  between 0.02 and 0.086, a linear approximation yields.

$$\epsilon_g^{(2)} \approx \frac{\epsilon_{pc}^{(2)}}{1.258} - 0.00067 \quad (4)$$

However, the radiative coupling between the patch and cone is about twice as large for the side areas of the second-stage patch. The sides have a surface area of 1.527 in<sup>2</sup> out of a total of 2.62 in<sup>2</sup>; their radiative coupling "weight" is therefore about

$$2 \times \frac{1.527}{1.093} = 2.794$$

The average weighting factor for the whole patch is then 1.397, and equation (4) becomes

$$\epsilon_g^{(2)} \approx \frac{1}{1.397} \left[ \frac{\epsilon_{pc}^{(2)}}{1.258} - 0.00067 \right] \quad (5)$$

The calculated values of  $\epsilon_g^{(2)}$  are given in Table 8 for the  $\epsilon_{pc}^{(2)}$  values of Table 7.

Table 8

Estimate of Cone Surface Emissivity in Second Stage

Space Reference Reflectivity	$\epsilon_g^{(2)}$
0.02	0.1036
0.05	0.0671
0.08	0.0291

Note that the range of calculated surface emissivities (3.6 to 1) is nearly as great as the range of space reference reflectivities (4 to 1). The above model yields a value of  $\epsilon_g^{(2)}$  within the range calculated for the first-stage cone (0.063 to 0.0773) only at a reference reflectivity of 5 percent.

## 2.4 Temperature Corrections for Imperfect Space Reference

The cold reference used during chamber tests of the two-stage radiant cooler does not provide a complete simulation of outer space. It is not sufficiently cold and does not have an absorptivity of unity. The reference attains a temperature of about 30 degrees K (Fifth Quarterly Report, Section 4.4) rather than the 4 degrees K of space, and its absorptivity is that of 3M Black Velvet (0.92 to 0.98). The higher temperature produces very small errors for a patch at liquid nitrogen temperature or above, but the lower absorptivity produces significant errors even in the temperature of the first-stage patch. It therefore becomes necessary to correct the patch temperatures measured in the space chamber for a nominal range of space reference reflectivities. Equations for the corrections are derived below and applied to the results of thermal test 7 (Section 2.2).

The absorptivity of the space reference can be increased by the use of cavities. For example, a reference covered with 30 degree triangular grooves decreases the reflectivity of the surface from the 2 to 8 percent range to 0.75 to 3.1 percent.

### 2.4.1 Space Reference Temperature

First we will show that a space reference temperature of 30 degrees K has only a very small influence on the temperature of the second-stage patch. The thermal-balance equation for the second-stage patch when viewing a black space reference at 0 degrees K is (First Quarterly Report, p. 54)

$$\sigma A_{p2} T_o^4 = \epsilon_{pc}^{(2)} \sigma A_{p2} T_{p1}^4 + K_c (T_{p1} - T_o) \quad (6)$$

where  $A_{p2}$  = radiating area of the second-stage patch

$T_o$  = temperature of the second-stage patch for a black space reference at 0 degrees K

$\epsilon_{pc}^{(2)}$  = effective patch-to-cone emissivity in the second stage

$T_{p1}$  = temperature of the first-stage patch

$K_c$  = conductive coupling coefficient between stages

If the same patch views a black space reference at a temperature  $T_r$  above absolute zero, the patch temperature is increased to  $T_{p2}$  and its thermal balance equation becomes

$$\sigma A_{p2} T_{p2}^4 = \epsilon_{pc}^{(2)} \sigma A_{p2} T_{p1}^4 + K_c (T_{p1} - T_{p2}) + (1 - \epsilon_{pc}^{(2)}) \sigma A_{p2} T_r^4 \quad (7)$$

This equation neglects the increase in first-stage temperature produced by the space reference. Subtracting equation (6) from equation (7), we obtain

$$\sigma A_{p2} (T_{p2}^4 - T_o^4) = A_{p2} \sigma T_r^4 - K_c (T_{p2} - T_o) \quad (8)$$

for  $\epsilon_{pc}^{(2)}$  much less than one (i. e. , neglecting absorption of reference radiation in the second-stage cone). This may be rearranged to give

$$T_{p2}^4 + \frac{K_c}{\sigma A_{p2}} T_{p2} = T_o^4 + T_r^4 + \frac{K_c}{\sigma A_{p2}} T_o \quad (9)$$

For  $K_c = 0.0339 \text{ mw/}^\circ\text{K}$  (Second Quarterly Report, Section 2.3)

$A_{p2} = 2.62 \text{ in}^2$  (Third Quarterly Report, p. 22)

$T_o = 75^\circ\text{K}$

$T_r = 30^\circ\text{K}$

equation (9) becomes

$$T_{p2}^4 + 3.538 \times 10^5 T_{p2} = 0.5899 \times 10^8 \text{ }^\circ\text{K}^4$$

The solution is

$$T_{p2} = 75.4^\circ\text{K} \quad (10)$$

This is an increase of only 0.4 degrees K or about 1/2 percent.

#### 2.4.2 Space Reference Reflectivity

The non-black space reference provides paths not present in outer space by which radiation from the first-stage cone and patch can reach the second-stage patch. Additional paths are also provided for radiative transfer from the first-stage cone and patch to the first-stage patch. The patch temperatures measured in the space chamber are therefore higher than those achieved in outer space and must be corrected to a condition of zero reference reflectivity. Procedures to determine these corrections are described below and applied to the results of thermal test 7. In the next section, we consider the use of cavities to reduce the reflectivity of the space reference and therefore the magnitude of the corrections required to estimate the in-orbit performance.

The radiant power from the first-stage patch diffusely reflected off the space reference is given by

$$\begin{aligned}\Phi_{p-r} &= \sigma A_{p1} T_{p1}^4 \rho_{pc} \rho_r (1 + \rho_r g_2 + \rho_r^2 g_2^2 + \dots) \\ \Phi_{p-r} &= \sigma A_{p1} T_{p1}^4 \frac{\rho_{pc} \rho_r}{1 - g_2 \rho_r}\end{aligned}\quad (11)$$

- where  $A_{p1}$  = radiating area of the first-stage patch
- $T_{p1}$  = temperature of the first-stage patch
- $\rho_{pc}$  = effective reflectivity of the first-stage cone for radiation from the first-stage patch (First Quarterly Report, Appendix II)
- $\rho_r$  = reflectivity of the space reference
- $g_2$  = fraction of diffuse radiation from the space reference that returns to the reference by reflection in the first-stage cone

Similarly, the power from the first-stage cone reflected off the space reference is given by

$$\Phi_{c-r} = A_c \sigma T_c^4 \frac{\epsilon_{cx} \rho_r}{1 - g_2 \rho_r} \quad (12)$$

- where  $A_c$  = inner surface area of first-stage cone
- $T_c$  = temperature of first-stage cone
- $\epsilon_{cx}$  = effective external emissivity of first-stage cone (First Quarterly Report, Appendix VIII)

The total radiant power reaching the second-stage patch from the first stage by way of the space reference is then

$$\Phi_{s1-p2} = g_o (\Phi_{p-r} + \Phi_{c-r}) \quad (13)$$

- where  $g_o$  = fraction of diffuse radiation from space reference that reaches second-stage patch directly and by reflection in second-stage cone

At the edge of the first-stage mouth,  $g_o$  is essentially zero. The cooler is designed so that the second-stage patch sees little or none of the first-stage cone either directly or by reflection in the second-stage cone (See First Quarterly Report, Appendix VI; Third Quarterly Report Section 4.1.2). At the center of the first-stage mouth,  $g_o$  was calculated as the average for right-circular cones having the geometries of the vertical and horizontal planes of the cooler according to

$$g_{oc} = \sum_n F_{r-p2}^n \rho_g^n \quad (14)$$

where  $F_{r-p2}^n$  = view factor from center of first-stage mouth (space reference) to second-stage patch as seen by  $n$  reflections in second-stage cone

$\rho_g$  = reflectivity of second-stage cone wall

We also have for the right-circular geometry

$$F_{r-p2}^n = \sin^2 \gamma_n - \sin^2 \gamma_{n-1} \quad (15)$$

where  $\gamma_n$  = angle from cooler axis to intersection of the  $n-1$  and  $n$  reflections of second-stage patch in second-stage cone

Values of  $\sin^2 \gamma_n$  were determined by means of scale drawings. The results are listed in Table 9.

Table 9

View Factor to First  $n-1$  Reflections of Second-Stage Patch

$n$	Vertical	$\sin^2 \gamma_n$	Horizontal
1	0.00024		0.0118
2	0.00228		0.0598
3	0.00470		0.0657
4	0.00582		-

The values of  $g_o$  at the center of the first-stage mouth were calculated for the vertical and horizontal geometries using  $\rho_g = 0.93$ . The results are listed in Table 10.

Table 10

Calculation of $g_{oc}$ for $\rho_g = 0.93$				
n	$F_{r-p2}^n$		$F_{r-p2}^n \rho_g^n$	
	Vertical	Horizontal	Vertical	Horizontal
0	0.00024	0.0118	0.00024	0.0118
1	0.00204	0.0480	0.00190	0.0446
2	0.00242	0.0059	0.00209	0.0051
3	0.00112	-	0.00090	-
$g_{oc}$ :			0.00513	0.0615

Using the average of the vertical and horizontal values, we obtain

$$g_{oc} = 0.0333 \quad (16)$$

In keeping with the geometry used to calculate the view factors, we assumed that  $g_o$  varies linearly along a radius of the mouth of a right-circular cone and goes to zero at the edge. The average value of  $g_o$  over the mouth (space reference) is then

$$g_o = \frac{1}{\pi r_o^2} \int_0^{2\pi} \int_0^{r_c} g_{oc} \left(1 - \frac{r}{r_o}\right) r dr d\theta \quad (17)$$

where  $r_o$  is the radius of the cone mouth and  $r, \theta$  are polar coordinates in the plane of the mouth. Integrating, we obtain

$$g_o = \frac{1}{3} g_{oc} = 0.0111 \quad (18)$$

In thermal test 7, the cooler attained the equilibrium temperatures shown in Table 11.

Table 11

## Results of Thermal Test 7

Member	Equilibrium Temperature ( $^{\circ}\text{K}$ )
Outer Box	298.5
First-Stage Cone	201.6
First-Stage Patch	108.3
Second-Stage Patch	80.2

For an average surface emissivity,  $\epsilon_g$ , of 0.063 on the first-stage cone, we also have (Fifth Quarterly Report, Tables 1 and 2)

$$\rho_{pc} = 1 - \epsilon_{pc} = 0.9465$$

$$\epsilon_{cx} = 0.0375$$

In addition,

$$A_{p1} = 70.23 \text{ in}^2 \text{ (Third Quarterly Report, p. 22)}$$

$$A_{c1} = 933 \text{ in}^2 \text{ (Second Quarterly Report, p. 5)}$$

$$g_2 = 0.5958 \text{ (Fifth Quarterly Report, p. 23)}$$

The radiant power from the first-stage reflected off the space reference was then (equations 11 and 12)

$$\Phi_{p-r} + \Phi_{c-r} = \frac{2448 \rho_r}{1 - 0.5958 \rho_r} \quad (19)$$

during thermal test 7. Values of this power are listed in Table 12 together with the power absorbed in the second-stage patch for  $g_o = 0.0111$ .

Table 12

#### Radiant Power Reflected from Space Reference

$\rho_r$	Total ( $\Phi_{p-r} + \Phi_{c-r}$ ), mw	To second-stage patch $g_o (\Phi_{p-r} + \Phi_{c-r})$ , mw
0.02	49.5	0.55
0.05	126.1	1.40
0.08	205.6	2.28

The power radiated by a black second-stage patch at 80.2 degrees K is

$$\Phi_{p2} = \sigma A_{p2} T_{p2}^4 = 3.96 \text{ milliwatts}$$

This power is balanced by radiative inputs from the second-stage cone and space reference and by a conductive input from the first-stage patch. The thermal-balance equation is therefore

$$3.96 \text{ mw} = \Phi_r + K_c (T_{p1} - T_{p2}) \quad (20)$$

where  $\Phi_r$  is the radiative input. The value of the conductive coupling coefficient,  $K_c$ , may be calculated from

$$K_c = \frac{1}{\ell} \sum A_i K_i \quad (21)$$

where  $\ell$  = length of conductive path between stages

$A_i$  = cross-sectional area of conductive member  $i$

$K_i$  = thermal conductivity of conductive member  $i$

The conductive members are listed in Table 13; all have a length,  $\ell$ , of 1.42 inches.

Table 13

Conductive Members Between Stages in Test 7

Material	Cross-sectional dimensions, inch	Thermal Conductivity watt/cm <sup>2</sup> C
chromel	$2 \times 10^{-3}$ dia.	0.200 @ 100 <sup>o</sup> K
constantan	$2 \times 10^{-3}$ dia.	0.192 @ 373 <sup>o</sup> K
nylon sleeve (2)	$3.1 \times 10^{-2}$ O. D. , $7.5 \times 10^{-3}$ wall	$3.1 \times 10^{-3}$ , average 20 <sup>o</sup> K - 300 <sup>o</sup> K
Synthane G-10	1/8 O. D. , 3/32 I. D.	$2.94 \times 10^{-3}$ @ 293 <sup>o</sup> K

We will assume the chromel and constantan have a conductivity of 0.200 watt/cm degrees C at the average temperature between stages and that the Synthane G-10 has a conductivity of  $2.94 \times 10^{-3}$  watt/cm degrees C at the same temperature. We then have

$$K_c = 0.0356 \text{ milliwatt/}^{\circ}\text{K} \quad (22)$$

For this value of conductive coupling, coefficient,  $T_{p1} = 108.3^{\circ}\text{K}$ , and  $T_{p2} = 80.2^{\circ}\text{K}$ , equation (20) yields

$$\Phi_r = 2.96 \text{ milliwatts} \quad (23)$$

By subtracting the radiant power from the space reference, we obtain the radiant power to the second-stage patch for outer-space operation (space reference reflectivity of zero). The results are shown in Table 14 for reference reflectivities of 2, 5, and 8 percent.



Table 14

Thermal Load on Second-Stage Patch for Reference Reflections to First Stage Only

$\rho_r$	Radiant Power from Second-Stage Cone to Second-Stage Patch (mw)
0.02	2.41
0.05	1.56
0.08	0.68

For the power levels of Table 14, a first-stage temperature of 108.3 degrees K, and  $K_c$  equal to 0.0356 mw/degrees K, equation (91) of the First Quarterly Report yields

$$0.0356 T_{p2} + 9.581 \times 10^{-8} T_{p2}^4 = \left\{ \begin{array}{l} 6.265 \\ 5.415 \\ 4.535 \end{array} \right\} \text{ milliwatts} \quad (24)$$

The values of power on the right-hand side of the equation are for reference reflectivities of 2, 5, and 8 percent, top to bottom.

Equation (24) was solved for the temperature ( $T_{p2}$ ) of the second-stage patch when no power is reflected off the space reference. The results are given in Table 15.

Table 15

Temperature of Second-Stage Patch for Reference Reflections to First-Stage Only

$\rho_r$	Temperature of Second-Stage Patch For No Interstage Coupling Via Space Reference ( $^{\circ}\text{K}$ )
0.02	77.7
0.05	73.5
0.08	68.4

The radiant power from the first stage reflected from the space reference and absorbed in a black first-stage patch is given by

$$\Phi_{s1-p1} = g_1 (\Phi_{p-r} + \Phi_{c-r}) \quad (25)$$

where  $g_1$  = fraction of diffuse radiation from space reference that reaches first-stage patch directly and by reflection in first-stage cone

From the Fifth Quarterly Report, Section 4.5

$$g_1 = 0.2856$$

Values of  $\Phi_{s1-p1}$  are listed in Table 16 for reference reflectivities of 2, 5, and 8 percent and the values of  $(\Phi_{p-r} + \Phi_{c-r})$  given in Table 12.

Table 16

Thermal Load on First-Stage Patch Reflected from Space Reference

$\rho_r$	Radiant Power from Space Reference to First-Stage Patch, mw
0.02	14.1
0.05	36.0
0.08	58.7

The power radiated by a black first-stage patch at 108.3 degrees K is

$$\Phi_{p1} = \sigma A_{p1} T_{p1}^4 = 353.3 \text{ milliwatts} \quad (26)$$

By subtracting the value of  $\Phi_{s1-p1}$  from  $\Phi_{p1}$ , we obtain the power to the first-stage patch for zero reflectivity. Equating the result to  $A_{p1} \sigma T_{p1}^4$  and solving for the new value of  $T_{p1}$ , we obtain the patch temperature for zero reference reflectivity (this procedure assumes only radiative coupling in the first stage). The results are shown in Table 17.

Table 17

Outer Space Temperature of First-Stage Patch

$\rho_r$	Temperature of First-Stage Patch for No Coupling Via Space Reference ( $^{\circ}\text{K}$ )
0.02	107.2
0.05	105.4
0.08	103.5

Finally, the corrected second-stage temperature (Table 15) were adjusted for the corrected first-stage temperature (Table 17). This was done in the same manner as the original corrections to the temperature of the second-stage patch. In this case, the thermal-balance equation yields

$$0.0356 T_{p2} + 9.581 \times 10^{-8} T_{p2}^4 = \left\{ \begin{array}{l} 6.130 \\ 5.152 \\ 4.252 \end{array} \right\} \text{ milliwatts} \quad (27)$$

The solutions to this equation are listed in Table 18.

Table 18

Outer Space Temperature of Second-Stage Patch

$\rho_r$	Temperature of Second-Stage Patch For No Coupling Via Space Reference ( $^{\circ}\text{K}$ )
0.02	77.1
0.05	72.1
0.08	66.6

2.4.3 Reduction of Temperature Corrections

The reflectivity of the space reference can be reduced by providing cavities in its surface. The cavities should cover most or all of the surface area so that little or no flat area is left. In addition, the cavities should be reasonably easy to make and designed so their shape is not significantly changed when painted. A surface covered with 30 degree (total angle) V-grooves is a good choice. Essentially all the surface area can be covered with cavities and the angle is not so narrow that paint filling is a problem. In addition, the absorptivity of a V-groove is essentially the same as that of a conical cavity of the same angle (See E. M. Sparrow and R. D. Cess, "Radiation Heat Transfer," Brooks/Cole Div. of Wadsworth, 1966, pp. 168-169).

According to E. W. Treuenfels (JOSA 53, 1162, 1963), the absorptivity of a V-groove of total angle  $\omega$  and surface absorptivity  $\epsilon_o$  is given by

$$\epsilon_c = \frac{\epsilon_o}{\epsilon_o + f_1 (1 - \epsilon_o)} \quad (28)$$

$$\text{where } f_1 = 1 - \frac{\pi - \omega}{4} \cos \frac{\omega}{2} \quad (29)$$

These equations are for a diffusely reflecting surface. Values of  $\epsilon_c$  are given in Table 19 for  $\omega$  equal to 30 degrees and  $\epsilon_o$  values of 0.98, 0.95, and 0.92 (reflectivities of 0.02, 0.05, and 0.08). Also shown are values of the cavity reflectivity,  $\rho_c = 1 - \epsilon_c$ .

Table 19

Properties of a 30° V-Groove Cavity

$\epsilon_0$	$\epsilon_c$	$\rho_c$
0.98	0.9925	0.0075
0.95	0.9810	0.0190
0.92	0.9690	0.0310

The values given in Table 19 are in good agreement (within  $\sim 0.001$ ) of the results shown in Figure 6-6 of Sparrow and Cess (op. cit.) and in Figure 9 of Sparrow and Lin ("Absorption of Thermal Radiation in V-Groove Cavities", U. of Minn. for NASA-Lewis, N62 10682, July 1962).

The use of a 30 degree groove therefore reduces the nominal 5 percent reflectivity of 3M Black Velvet to 1.9 percent. This reduces the nominal total temperature correction for the second-stage patch from 8.1 degrees K to about 3.1 degrees K.

### 3.0 BREADBOARD RADIOMETER

Construction of the working breadboard radiometer (Phase III of the program) was started during the sixth quarter. The required characteristics are listed in Table 20.

Table 20

#### Required Radiometer Characteristics

Spectral region (-6 db points)	10.5 to 12.5 microns, $\pm 0.1$ micron
Collecting aperture diameter	5 inches maximum
Instantaneous field- of-view (-6 db points)	$2.5 \pm 0.2$ mr x $2.5 \pm 0.2$ mr
Noise equivalent temperature	Below $170^{\circ}\text{K}$
Noise equivalent temperature difference	Less than $2^{\circ}\text{K}$ at $220^{\circ}\text{K}$
Chopping frequency and electronic bandwidth	For contiguous subpoint scanning from 750 n mi.

The components to be added to the two-stage radiant cooler are the scan head (Section 3.1), relay optics (Section 3.2), and radiometer electronics (Section 3.3). Electrical and thermal test instruments (Section 3.4) will be used to measure the performance of the complete radiometer.

#### 3.1 Scan Head

The scan head of the breadboard radiometer is shown in Figure 6. It consists of a drive motor, gear box, casting, scan mirror, primary telescope, and mechanical chopper. The drive motor is a Bodine model 246 lubricated with low vapor pressure silicone grease (General Electric Versilube G-300). The output of the gear box drives the scan mirror and chopper through flexible couplings. The primary telescope is a 4-inch diameter f/1 parabola and a 2.4-inch diameter folding flat.

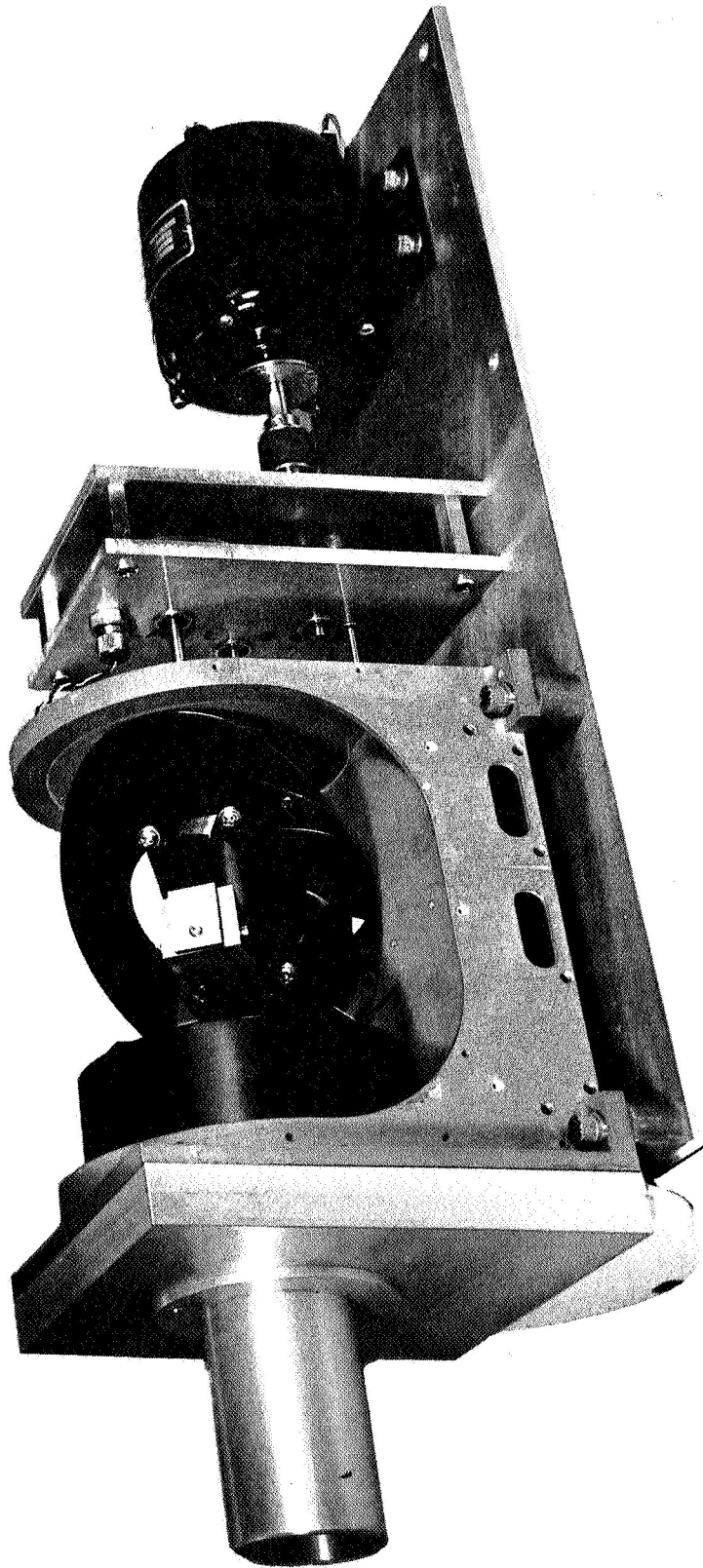


Figure 6 Radiometer Scan Head

For contiguous scan lines at the subpoint from an altitude of 750 n mi, the scan mirror must rotate at 100 rpm when the instantaneous field-of-view in 2.5 milliradians (First Quarterly Report, Section 6.0). The electronic post-demodulation bandwidth is then 2100 hz. The chopping frequency must exceed twice this value; a rate of 6000 hz was selected. For a chopper with 180 teeth, the corresponding chopper wheel rotational rate is 2000 rpm.

### 3.2 Relay Optics

The design data for the relay optics are given in Table 21, and the mechanical assembly is shown in Figure 7. The clear apertures listed in the table are those of the axial beam. Minimum clear apertures for no vignetting over the field-of-view in the presence of decentering and tilting are listed in Table 8 of the Second Quarterly Report. Three of these apertures had to be increased as a result of an increase in the cone-to-patch gap in the second stage (Fourth Quarterly Report, Table 8).

Table 21

#### Relay Optics Design

Element	Radius	Separation/Thickness	Material	Aperture Radius
2	{ -0.827 -0.9199	0.6507	Vacuum	
		0.311	Ge	0.38
				0.52
3	{ -6.235 -3.646	0.2297	Vacuum	
		0.300	Ge	0.61
				0.64
4	{ 30.03 $\infty$	6.000	Vacuum	
		0.300	Ge	0.65
				0.64
7	{ 0.2519685 0.1889764	7.911	Vacuum	
		0.1259842	Ge	0.14
				0.08
		0.189	Vacuum	

Element	Description
①	Chopper (Primary Focus)
② & ③	Collimating Lens
④	f/8 Focusing Lens
⑤	45° Folding Flat
⑥	10.5 - 12.5 Micron Filter
⑦	Aplanatic Lens
⑧	Infrared Detector (Secondary Focus)

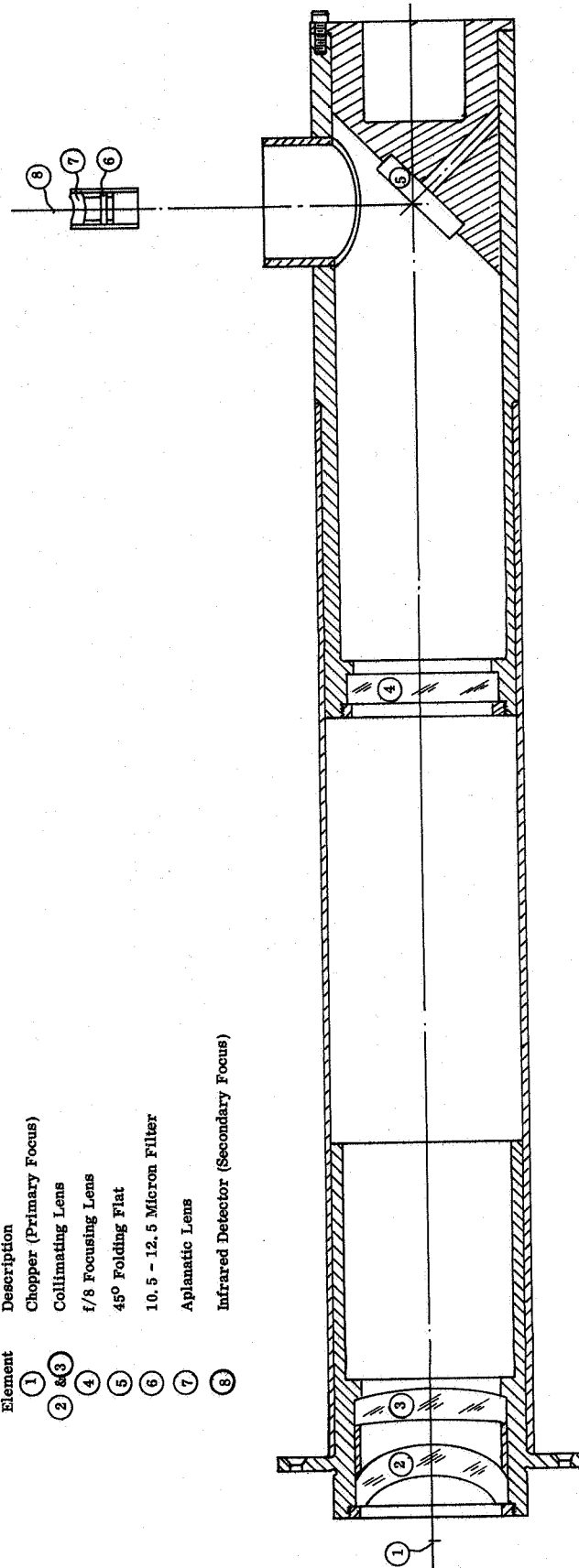


Figure 7 Relay Optics Assembly



The first two germanium elements in the relay optics (very nearly) collimate the  $f/1$  beam from the 0.25 mm square primary image at the chopper plane. The last two germanium elements, the  $f/8$  focusing and aplanatic lenses refocus the radiation on the 0.5 mm square infrared detector at the secondary focus. The  $f/8$  lens is described in Section 5.0 of the Fifth Quarterly Report and the aplanatic lens in Section 5.1 of the Fourth Quarterly Report. The spectral response is determined by the 10.5 to 12.5 micron interference filter (Fourth Quarterly Report, Figure 19). The filter and aplanatic are mounted within the first-stage patch (Fourth Quarterly Report, Figure 13).

The relay optics magnify the 4 inch focal length of the primary telescope by 2X. When combined with the infrared detector of sensitive area 0.553 mm x 0.449 mm, the nominal instantaneous field-of-view is then 2.6 mr x 2.2 mr.

### 3.3 Electronics

The signal from the infrared detector will be fed to a transistor preamplifier manufactured by Perry Associates, Brookline, Mass. The specifications for the preamplifier are given in Table 22 and the broadband noise performance in Figure 8. The device is specifically designed to match the low impedance of the infrared detector (50 to 200 ohms) while preserving low noise performance without the aid of an input transformer or other inductive component. The signal from the preamplifier will be fed to the video electronics described in Section 6.0 of the Fifth Quarterly Report. The preamplifier and video amplifier, plus the chopper and mirror pickoffs, will be mounted in the space chamber. The remainder of the electronics will be housed outside the chamber with the electronic test equipment (Figure 10).

Table 22

#### Preamplifier Specifications (Perry Model 600)

Gain ( $R_g = 50$ )	-----	40 db
Bandwidth ( $R_g = 100$ )	-----	20 cps to 100 kc
Band Flatness	-----	1 db
Noise Figure (Broadband, $R_g = 100$ )	-----	2 db
Input Impedance	-----	50 ohms
Output Impedance ( $F = 1$ kc)	-----	500 ohms
Output Level Maximum	-----	1 volt rms
Operating Temperature	-----	-55° to +125°C
Power Requirements	-----	±12 volts 6 ma
Mechanical Size	-----	2" x 2" x 1"

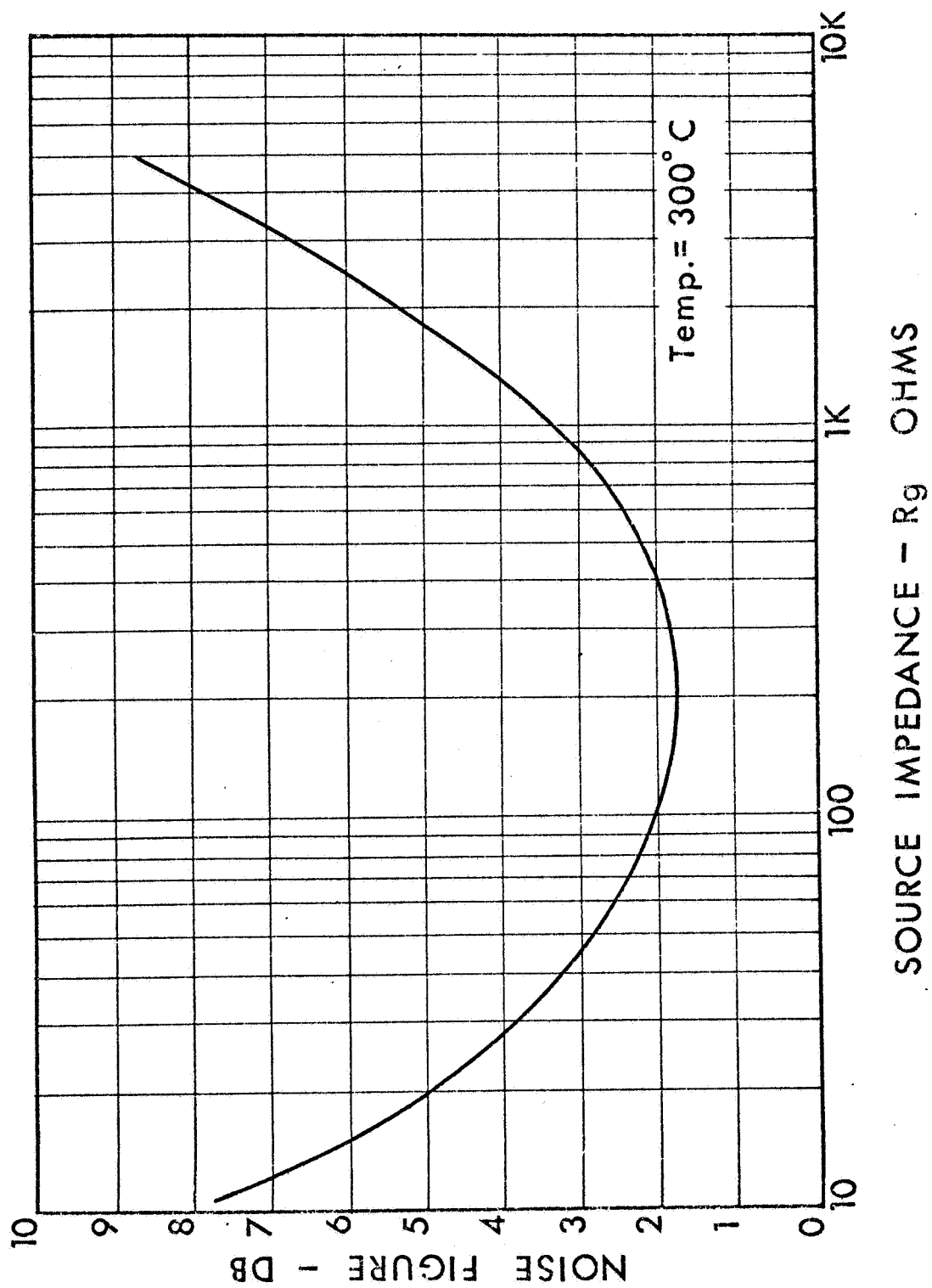


Figure 8 Preamplifier Broadband Noise Performance

### 3.4 Test Equipment

A block diagram of the test equipment for the breadboard radiometer is shown in Figure 9. The test instrumentation is described in Section 4.0 of the Second Quarterly Report and Section 3.0 of the Fifth Quarterly Report. The automatic control unit originally designed for the thermoelectric baseplate was modified to regulate the temperature of the radiometer calibration target.

A photograph of the electronic test equipment is shown in Figure 10. The cabinets contain the instruments listed in Table 23.

Table 23

#### Electronic Test Equipment

Cabinet 1	Cabinet 2	Cabinet 3
Honeywell Elektronik Multichannel Recorder	Patch Panel	Secondary Voltage Standard
Low Temperature Monitor Unit	Breadboard Electronics (Partial*)	Digital Voltmeter
Calibration Target Temperature Control		Oscilloscope
Variacs for Motor Power and Target Heater		Digital Printer
Primary 24 vdc Power Supply		Honeywell 1508 Visicorder
		Galvanometer Amplifiers (6)

An extended aluminum shroud was constructed to provide a cold space look for the breadboard radiometer. The portion facing the scanner (rather than the copper structure) was painted with 3M Black Velvet. The outer surface of the aluminum is covered with aluminized mylar to offset the thermal loading on the black area and thus maintain the aluminum at a temperature of 100 degrees K or less. Figure 11 shows the shroud and the calibration blackbody target mounted in the space chamber.

---

\* Remainder is in space chamber

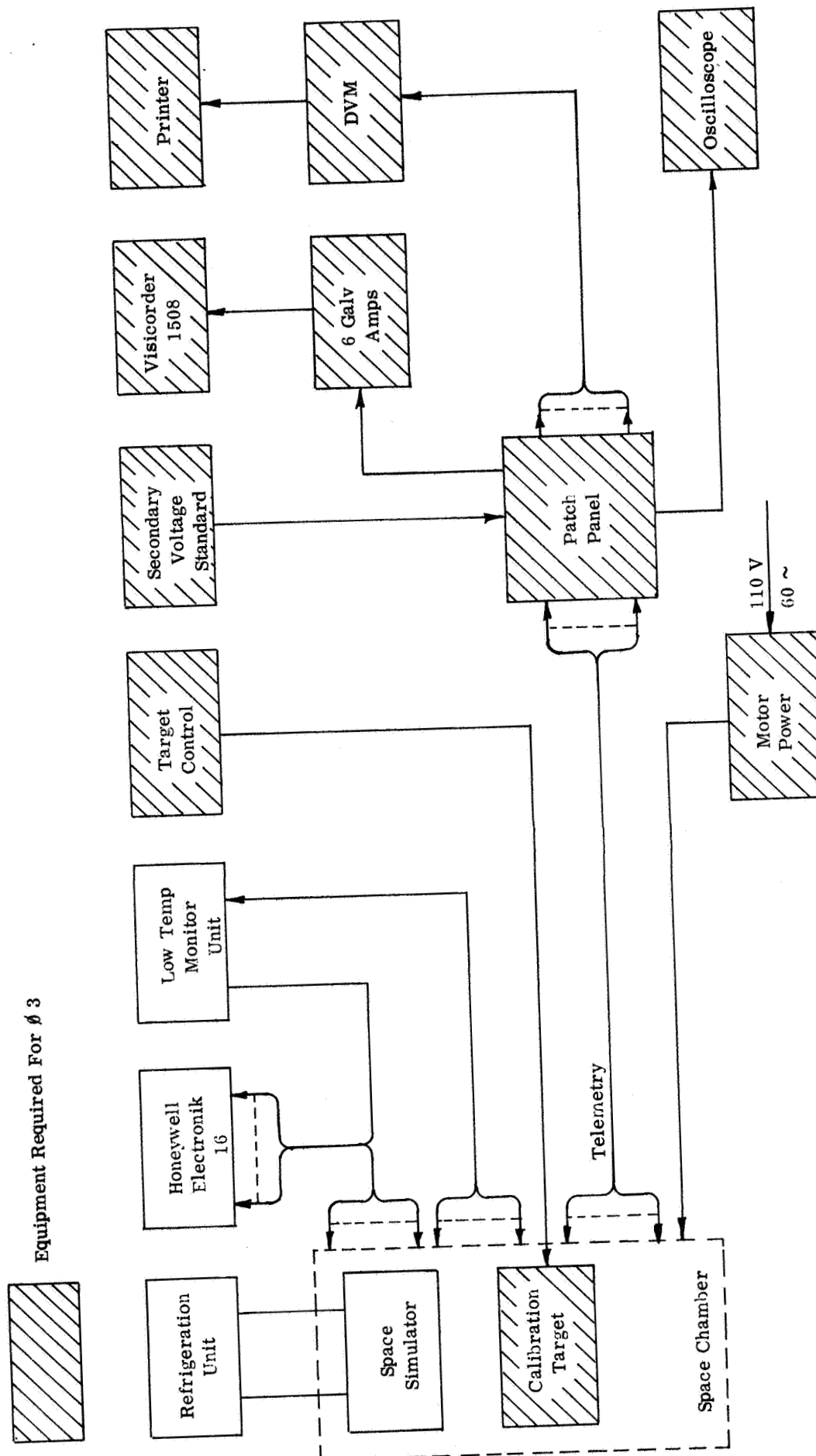


Figure 9 Test Equipment Block Diagram

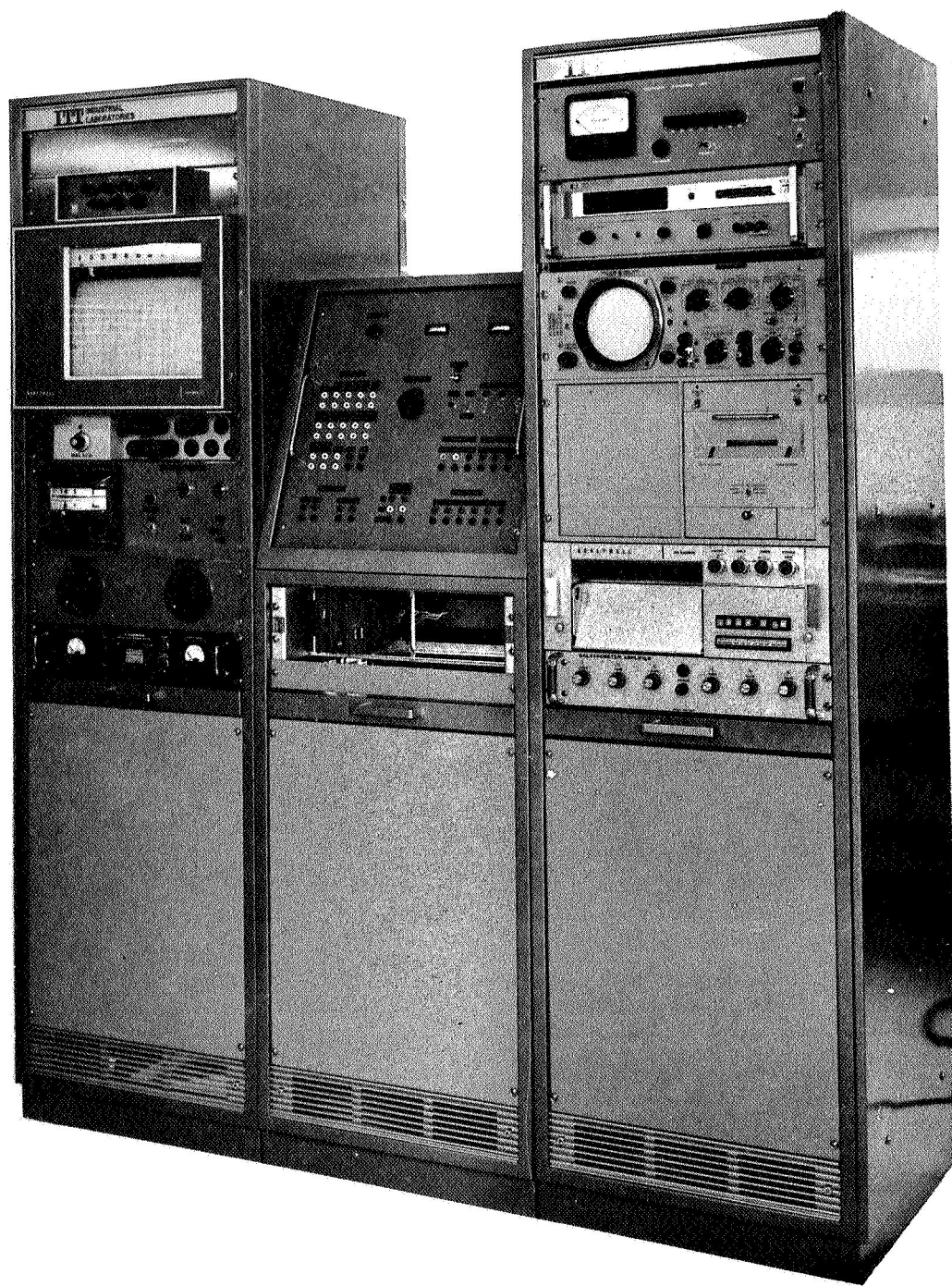


Figure 10 Electronic Test Equipment

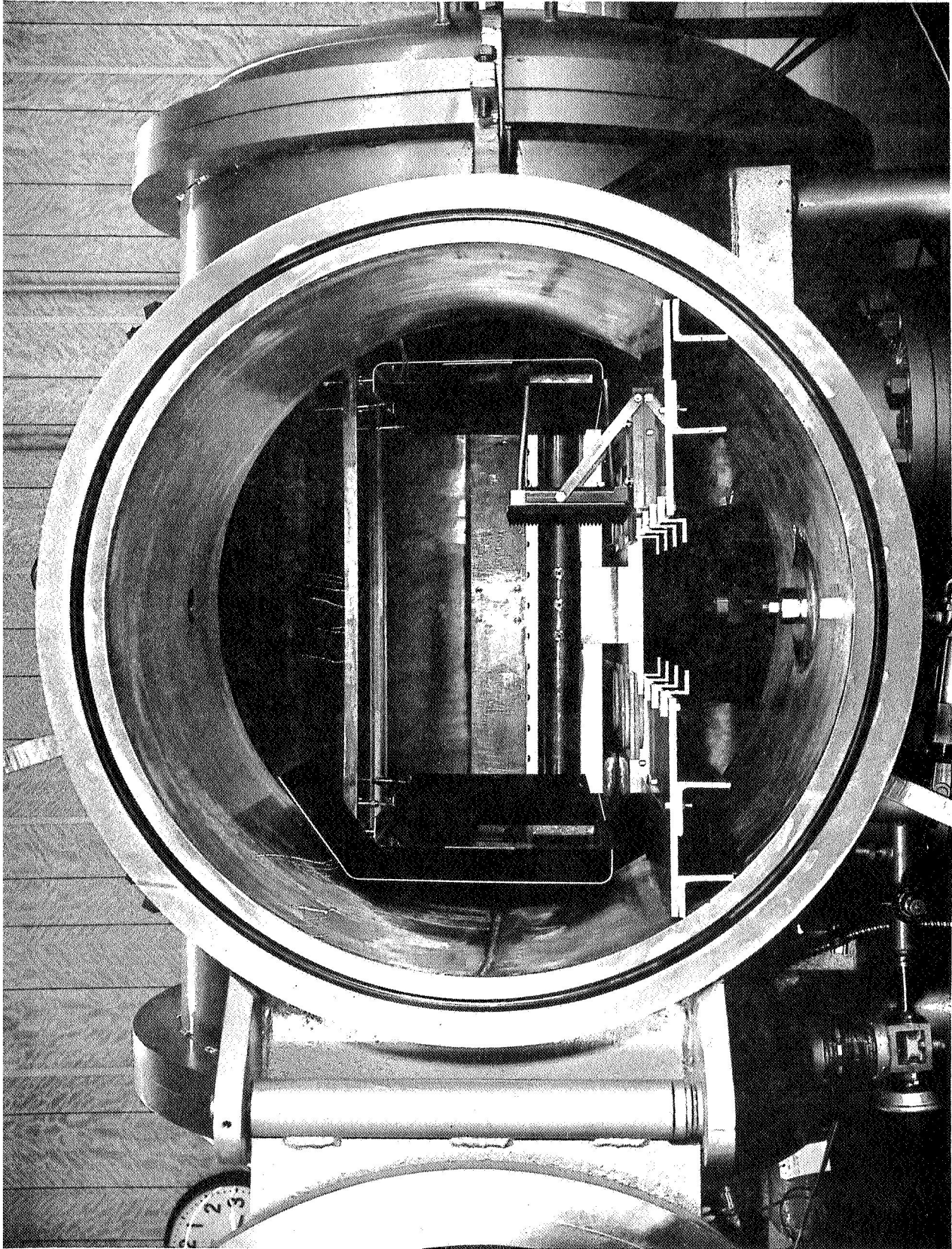


Figure 11 Space Scan and Calibration Targets in Space Chamber

#### 4.0 NEW TECHNOLOGY

No items which are considered new technology according to the NASA New Technology clause of September 1964 were developed during the sixth quarter. However, the feasibility of the two-stage radiant cooler (First Quarterly Report, Section 7.0) was demonstrated.

## 5.0 PROGRAM FOR NEXT QUARTER

We plan to complete the project by 30 November 1967. During the next two months, the scan head, relay optics, and electronics will be integrated with the two-stage radiant cooler into a working breadboard radiometer. The radiometer will be tested and a data booklet prepared. The final project report will then be written.



## 6.0 CONCLUSIONS AND RECOMMENDATIONS

The thermal tests performed during the sixth quarter demonstrated the feasibility of the two-stage radiant cooler. A second-stage temperature below 80 degrees K can be realized under realistic thermal load conditions. Realistic mechanical conditions in critical cooler parts have already been established (Fifth Quarterly Report, Sections 2.0 and 9.0).

A radiant cooler and a fast, sensitive infrared detector are the basic components in a family of infrared space instruments covering the wavelength region from the visible to 15 microns. The higher wavelengths are covered by a two-stage radiant cooler with a second-stage temperature below 80 degrees K and a  $\text{Hg}_{1-x}\text{Cd}_x\text{Te}$  detector (P. W. Kruse, Appl. Opt. 4, 68, 1965; C. Verié and J. Ayas, Appl. Phys. Lett. 10, 241, 1 May 1967).

The accuracy of simulating outer space operation of the two-stage radiant cooler is presently limited by the reflection of radiation from the flat cold space reference. The maximum reference temperature of 30 degrees K is sufficiently low and introduces a much smaller error (0.4 degrees K in a second-stage at 75 degrees K). We therefore recommend the use of a cavity or series of cavities to enhance the absorptivity of the space reference and reduce the necessary temperature corrections.